

## Protonation of Carbon Single-Walled Nanotubes Studied Using $^{13}\text{C}$ and $^1\text{H}$ - $^{13}\text{C}$ Cross Polarization Nuclear Magnetic Resonance and Raman Spectroscopies

Chaiwat Engtrakul,<sup>\*,†</sup> Mark F. Davis,<sup>\*,‡</sup> Thomas Gennett,<sup>§</sup> Anne C. Dillon,<sup>†</sup>  
Kim M. Jones,<sup>||</sup> and Michael J. Heben<sup>†</sup>

Contribution from the Center for Basic Sciences, National Renewable Energy Laboratory, Golden, Colorado 80401, National Bioenergy Center, National Renewable Energy Laboratory, Golden, Colorado 80401, Chemistry Department, Rochester Institute of Technology, Rochester, New York 14623, and National Center for Photovoltaics, National Renewable Energy Laboratory, Golden, Colorado 80401

Received August 23, 2005; E-mail: chaiwat\_engtrakul@nrel.gov; mark\_davis@nrel.gov

**Abstract:** The reversible protonation of carbon single-walled nanotubes (SWNTs) in sulfuric acid and Nafion was investigated using solid-state nuclear magnetic resonance (NMR) and Raman spectroscopies. Magic-angle spinning (MAS) was used to obtain high-resolution  $^{13}\text{C}$  and  $^1\text{H}$ - $^{13}\text{C}$  cross polarization (CP) NMR spectra. The  $^{13}\text{C}$  NMR chemical shifts are reported for bulk SWNTs,  $\text{H}_2\text{SO}_4$ -treated SWNTs, SWNT-Nafion polymer composites, SWNT-AQ55 polymer composites, and SWNTs in contact with water. Protonation occurs without irreversible oxidation of the nanotube substrate via a charge-transfer process. This is the first report of a chemically induced change in a SWNT  $^{13}\text{C}$  resonance brought about by a reversible interaction with an acidic proton, providing additional evidence that carbon nanotubes behave as weak bases. Cross polarization was found to be a powerful technique for providing an additional contrast mechanism for studying nanotubes in contact with other chemical species. The CP studies confirmed polarization transfer from nearby protons to nanotube carbon atoms. The CP technique was also applied to investigate water adsorbed on carbon nanotube surfaces. Finally, the degree of bundling of the SWNTs in Nafion films was probed with the  $^1\text{H}$ - $^{13}\text{C}$  CP-MAS technique.

### 1. Introduction

Nuclear magnetic resonance (NMR) spectroscopy has the potential to be a powerful tool in the structural, chemical, and electronic characterization of carbon single-wall nanotubes (SWNTs), their derivatives, and nanotube-based materials. NMR has been used extensively to characterize fullerenes<sup>1</sup> and their derivatives,<sup>2</sup> but the application of NMR spectroscopy to nanotubes has been more difficult with substantial progress being made only in the last several years. Unlike the small fullerenes (e.g.,  $\text{C}_{60}$ ,  $\text{C}_{70}$ , etc.), which can be readily isolated through differences in solubility or vapor pressure,<sup>2</sup> SWNTs possess a large polydispersity in diameter, chirality, and length and are difficult to separate from the carbonaceous and catalytic metal impurities that are coproduced during synthesis.<sup>3</sup> Advances in SWNT purification have allowed for the observation of the  $^{13}\text{C}$  resonance for SWNT nuclei by solid-state NMR, but the full power of NMR spectroscopy to follow chemical

reactions, characterize conformational and dynamic processes, and probe interfacial phenomena on the nanoscale remains to be realized.<sup>4</sup> A fully developed suite of NMR spectroscopies will aid in understanding the chemical reactivity and adsorptive behavior of SWNTs and the degree to which SWNTs interact with surrounding media, such as in polymer composites. Such an understanding will be essential for effectively manipulating and processing these materials for a wide array of potential applications.<sup>5</sup>

Solid-state  $^{13}\text{C}$  NMR spectroscopy with magic-angle spinning (MAS) has been applied to the characterization of neat SWNTs<sup>6–8</sup> and their derivatives.<sup>9–15</sup> Several of these studies have probed the chemical behavior of SWNTs and provided

<sup>†</sup> Center for Basic Sciences, National Renewable Energy Laboratory.

<sup>‡</sup> National Bioenergy Center, National Renewable Energy Laboratory.

<sup>§</sup> Rochester Institute of Technology.

<sup>||</sup> National Center for Photovoltaics, National Renewable Energy Laboratory.

(1) Johnson, R. D.; Meijer, G.; Bethune, D. S. *J. Am. Chem. Soc.* **1990**, *112*, 8983–8984.

(2) Buhl, M.; Hirsch, A. *Chem. Rev.* **2001**, *101*, 1153–1183.

(3) Saito, R.; Dresselhaus, G.; Dresselhaus, M. S. *Physical Properties of Carbon Nanotubes*; Imperial College Press: London, 1998.

(4) Brown, S. P.; Spiess, H. W. *Chem. Rev.* **2001**, *101*, 4125–4155.

(5) Dai, H. *Acc. Chem. Res.* **2002**, *35*, 1035–1044.

(6) Tang, X. P.; Kleinhannes, A.; Shimoda, H.; Fleming, L.; Bennoune, K. Y.; Sinha, S.; Bower, C.; Zhou, O.; Wu, Y. *Science* **2000**, *288*, 492–494.

(7) Hayashi, S.; Hoshi, F.; Ishikura, T.; Yumura, M.; Ohshima, S. *Carbon* **2003**, *41*, 3047–3056.

(8) Goze-Bac, C.; Latil, S.; Vaccarini, L.; Bernier, P.; Gaveau, P.; Tahir, S.; Micholet, V.; Aznar, R.; Rubio, A.; Metenier, K.; Beguin, F. *Phys. Rev. B* **2001**, *63*, 100302.

(9) Goze-Bac, C.; Latil, S.; Lauginie, P.; Jourdain, V.; Conard, J.; Duclaux, L.; Rubio, A.; Bernier, P. *Carbon* **2002**, *40*, 1825–1842.

(10) Goze-Bac, C.; Bernier, P.; Latil, S.; Jourdain, V.; Rubio, A.; Jhang, S. H.; Lee, S. W.; Park, Y. W.; Holzinger, M.; Hirsch, A. *Curr. Appl. Phys.* **2001**, *1*, 149–155.

(11) Cahill, L. S.; Yao, Z.; Adronov, A.; Penner, J.; Moonosawmy, K. R.; Kruse, P.; Goward, G. R. *J. Phys. Chem. B* **2004**, *108*, 11412–11418.

(12) Peng, H. Q.; Alemany, L. B.; Margrave, J. L.; Khabashesku, V. N. *J. Am. Chem. Soc.* **2003**, *125*, 15174–15182.

evidence for the covalent functionalization of nanotube sidewalls.<sup>9–12</sup> For example, Peng et al. studied carboxylic acid functionalized materials by NMR, FTIR, Raman spectroscopy, transmission electron microscopy, and thermal gravimetric analysis and were able to assign a 2–3 ppm shift to lower frequency of the <sup>13</sup>C NMR resonance to chemical functionalization of nanotubes.<sup>12</sup> Cahill et al. used solid-state multidimensional NMR spectroscopy to demonstrate that polymerization initiators were associated with the surface of the carbon nanotubes.<sup>11</sup> Previous theoretical work has indicated that high-resolution <sup>13</sup>C NMR can distinguish between semiconducting and metallic SWNTs on the basis of a calculated 11 ppm difference in their chemical shifts.<sup>9,16</sup> In fact, on the basis of a recent density-functional study, it may be possible for NMR spectroscopy to identify the influence of the tube diameter and helicity on the <sup>13</sup>C NMR chemical shifts.<sup>17</sup> Most recently, Kitaygorodskiy et al. detected SWNT resonances for poly-(ethylene glycol)-functionalized carbon nanotubes, which were assigned to nanotube carbons on semiconducting and metallic SWNTs.<sup>14</sup>

The chemistry of SWNT surfaces is difficult to study by NMR due to magnetic and carbonaceous impurities that may be present in samples. Also, intended chemical reactions may occur equally as well on nanotube carbons and nonnanotube carbonaceous impurities, and aggressive chemical functionalization may convert the former into the latter. Consequently, the observation of the formation of a functional group in a nanotube sample upon chemical treatment is not clear evidence that the group is in fact associated with the nanotube.<sup>11</sup> To permit more straightforward interpretation of NMR data it is useful to start with rigorously pure and well-characterized samples and to focus on a relatively simple, nondestructive nanotube chemical reaction that can be directly followed by Raman spectroscopy. Superacids, such as sulfuric acid and chlorosulfonic acid, have been shown to delaminate SWNT bundles and solubilize SWNTs in significant quantities by protonation of nanotube sidewalls.<sup>18,19</sup> Protonation of SWNT materials has been investigated with Raman spectroscopy<sup>18,20–22</sup> and X-ray scattering experiments.<sup>23,24</sup> Ramesh et al. studied the interaction of SWNTs with several superacids and described protonation as a charge-transfer

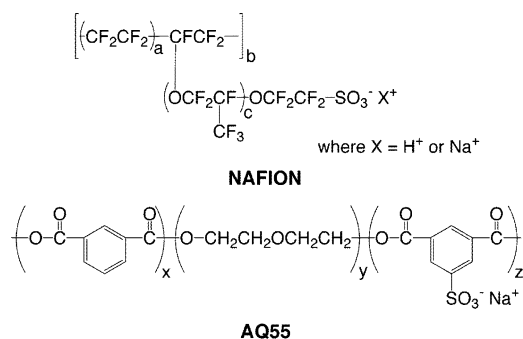


**Figure 1.** Polymer structures of the Nafion and Eastman AQ55 complexes. In Nafion, X is either a H<sup>+</sup> in the acid form or a Na<sup>+</sup> in the neutralized form.

process in which a C:H<sup>+</sup> moiety is formed due to a local perturbation of electronic charge from the nanotube in response to the proton.<sup>18</sup> The fractional removal of electrons from the SWNTs represents a polarization in the C:H<sup>+</sup> moiety without the formation of new covalent bonds. This protonation is completely reversible and does not result in a permanent change in nanotube structure or the permanent removal of electrons.

In this report we explore the use of solid-state <sup>13</sup>C and <sup>1</sup>H–<sup>13</sup>C cross polarization (CP) NMR spectroscopies to study the reversible protonation of highly pure SWNTs in sulfuric acid and by the extremely acidic sulfonate exchange sites (pK<sub>a</sub> ~ –6)<sup>25,26</sup> in the perfluorosulfonated polymer Nafion (Figure 1). Nafion has been recently found to disperse SWNTs, presumably by protonation, in similarity to sulfuric acid.<sup>27,28</sup> We focus on <sup>13</sup>C-based NMR techniques because interpretation of our initial <sup>1</sup>H NMR experiments were complicated by broad line widths due to bulk water effects. We followed the well-known affects of protonation on the electronic properties of SWNTs by Raman spectroscopy and correlated these findings with the NMR results. Prior to protonation, high-resolution spectra of pristine <sup>13</sup>C isotope-labeled SWNTs were obtained. The <sup>13</sup>C SWNT resonance was observed to be sensitive to the pH of the surrounding media and moved to higher frequency with protonation. The protonation was reversed, and the <sup>13</sup>C resonance returned to its initial position upon neutralization with base. Thus, this study presents the first clear observation of a chemically induced change in a SWNT <sup>13</sup>C resonance, brought about in this case by reversible protonation. Additionally, the CP technique was found to be a sensitive probe of the interactions between protons and SWNT <sup>13</sup>C nuclei. Magnetization transfer from protons to nanotube carbons was even observed from water molecules that were weakly interacting with the SWNT surfaces. The efficiency of the CP technique was demonstrated by investigating the <sup>1</sup>H–<sup>13</sup>C CP-MAS spectra of SWNTs dispersed in a sulfonated polyester analogue to Nafion, Eastman AQ55 (Figure 1). These latter experiments confirmed the role of pH in producing the chemical shift for the SWNT <sup>13</sup>C nuclei and ruled out the possibility of the change in resonance being due to wrapping of the hydrophobic portion of the polymers around the SWNTs. The degree of bundling was inferred from the full-width at half-

- (13) Schmid, M.; Goze-Bac, C.; Mehring, M.; Roth, S.; Bernier, P. <sup>13</sup>C NMR investigation of the metallic state of Li intercalated carbon nanotubes. *AIP Conf. Proc.* **2003**, 131–134.
- (14) Kitaygorodskiy, A.; Wang, W.; Xie, S. Y.; Lin, Y.; Fernando, K. A. S.; Wang, X.; Qu, L.; Chen, B.; Sun, Y. *P. J. Am. Chem. Soc.* **2005**, 127, 7517–7520.
- (15) Shimoda, H.; Gao, B.; Tang, X. P.; Kleinhammes, A.; Fleming, L.; Wu, Y.; Zhou, O. *Phys. Rev. Lett.* **2002**, 88, 015502.
- (16) Latil, S.; Henrard, L.; Bac, C. G.; Bernier, P.; Rubio, A. *Phys. Rev. Lett.* **2001**, 86, 3160–3163.
- (17) Zurek, E.; Autschbach, J. *J. Am. Chem. Soc.* **2004**, 126, 13079–13088.
- (18) Ramesh, S.; Ericson, L. M.; Davis, V. A.; Saini, R. K.; Kittrell, C.; Pasquali, M.; Billups, W. E.; Adams, W. W.; Hauge, R. H.; Smalley, R. E. *J. Phys. Chem. B* **2004**, 108, 8794–8798.
- (19) Davis, V. A.; Ericson, L. M.; Parra-Vasquez, A. N. G.; Fan, H.; Wang, Y. H.; Prieto, V.; Longoria, J. A.; Ramesh, S.; Saini, R. K.; Kittrell, C.; Billups, W. E.; Adams, W. W.; Hauge, R. H.; Smalley, R. E.; Pasquali, M. *Macromolecules* **2004**, 37, 154–160.
- (20) Zhou, W.; Vavro, J.; Guthy, C.; Winey, K. I.; Fischer, J. E.; Ericson, L. M.; Ramesh, S.; Saini, R.; Davis, V. A.; Kittrell, C.; Pasquali, M.; Hauge, R. H.; Smalley, R. E. *J. Appl. Phys.* **2004**, 95, 649–655.
- (21) Zhou, W.; Vavro, J.; Nemes, N. M.; Fischer, J. E.; Borondics, F.; Kamaras, K.; Tanner, D. B. *Phys. Rev. B* **2005**, 71, 205423.
- (22) Strano, M. S.; Huffman, C. B.; Moore, V. C.; O’Connell, M. J.; Haroz, E. H.; Hubbard, J.; Miller, M.; Rialon, K.; Kittrell, C.; Ramesh, S.; Hauge, R. H.; Smalley, R. E. *J. Phys. Chem. B* **2003**, 107, 6979–6985.
- (23) Zhou, W.; Heiney, P. A.; Fan, H.; Smalley, R. E.; Fischer, J. E. *J. Am. Chem. Soc.* **2005**, 127, 1640–1641.
- (24) Zhou, W.; Fischer, J. E.; Heiney, P. A.; Fan, H.; Davis, V. A.; Pasquali, M.; Smalley, R. E. *Phys. Rev. B* **2005**, 72, 045440.

- (25) Mauritz, K. A.; Moore, R. B. *Chem. Rev.* **2004**, 104, 4535–4585.
- (26) Petersen, M. K.; Wang, F.; Blake, N. P.; Metiu, H.; Voth, G. A. *J. Phys. Chem. B* **2005**, 109, 3727–3730.
- (27) Landi, B. J.; Raffaele, R. P.; Heben, M. J.; Alleman, J. L.; VanDerveer, W.; Gennett, T. *Nano Lett.* **2002**, 2, 1329–1332.
- (28) Liu, P.; Lee, S. H.; Yan, Y. F.; Gennett, T.; Landi, B. J.; Dillon, A. C.; Heben, M. J. *Electrochem. Solid-State Lett.* **2004**, 7, A421–A424.

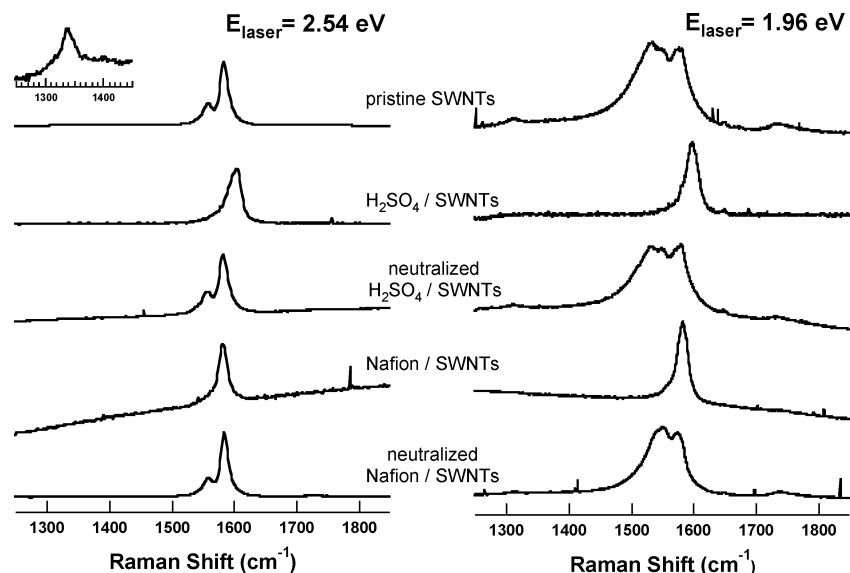


**Figure 2.** Raman spectra obtained at 2.54 eV (left panel) and 1.96 eV (right panel) for pristine SWNTs, SWNTs protonated by  $\text{H}_2\text{SO}_4$  before and after neutralization in NaOH, SWNT–Nafion composites, and neutralized SWNT–Nafion composites. The inset shows the Raman spectrum of the D-band at an expanded scale at 2.54 eV excitation for pristine SWNTs. The Raman spectra are normalized to the intensity of the G-band peak.

maximum (fwhm) of the carbon nanotube resonances for the different SWNT–polymer composites.

## 2. Experimental Section

**2.1. General Methods.** The  $^{13}\text{C}$  isotope-labeled SWNT materials used in this study were synthesized by a modified laser vaporization method<sup>29</sup> similar to that of Thess et al.<sup>30</sup> Targets were made by pressing powdered graphite ( $\sim 1\ \mu\text{m}$  particle size) mixed with 20 wt % amorphous carbon ( $^{13}\text{C}$ , 99%, Cambridge Isotope Laboratories, Inc.) doped with 0.6 at. % each Co and Ni at 10,000 psi in a 1 in. die. Laser-generated SWNTs typically have low defect densities, making them easier to purify and relatively unreactive during the reflux or oxidation processes.<sup>29</sup> The raw SWNT soot was collected, and the metal catalyst and carbonaceous impurities were removed using a purification method similar to that of Dillon et al.<sup>29</sup> that produces SWNT materials with >95 wt % purity. The purification procedure was altered slightly by rinsing the isolated nitric acid refluxed SWNT material with alternating aliquots of acetone and water until the filtrate became colorless. The SWNT material was then oxidized in  $\text{CO}_2$  flowing at 100 sccm in a tube furnace at 825 °C for 1 h rather than in air.<sup>31</sup> This final step burned off the reactive nonnanotube carbon impurities and left the sample rigorously dry. On the basis of Raman scattering measurements in Figure 2, the SWNT materials were  $\sim 20\%$   $^{13}\text{C}$  enriched according to the shift in the G-band.<sup>32</sup> All purified SWNT materials and SWNT–polymer composites were stored in an oxygen-free atmosphere.

NMR samples were prepared in a glovebox under a helium atmosphere. The SWNT materials ( $\sim 0.5\ \text{mg}$ ) were loaded into silicon nitride rotors (7 mm outer diameter) and packed between two plugs of either polyethylene or Teflon to balance the rotor, center the small amount of sample in the NMR coil, and provide a barrier against exposure to ambient conditions. Polyethylene plugs were used in single pulse experiments and Teflon plugs in CP experiments to minimize background signals. Adamantane was added as an internal reference to aid in setting the Hartmann–Hahn match condition in CP experi-

ments where probe tuning was significantly affected by the introduction of the nanotube materials into the NMR coil. Samples were transferred in a helium bag directly to the NMR spectrometer. High-resolution, solid-state  $^{13}\text{C}$  NMR spectra were collected on a Bruker Avance 200 MHz spectrometer (4.7 T) operating at 50.13 MHz for  $^{13}\text{C}$  at room temperature, with MAS rotation rates of 6 or 7 kHz under a nitrogen atmosphere. The spectra were acquired under high-power proton decoupling using a  $\pi/2$  pulse length of 6.6  $\mu\text{s}$  and a recycle delay of 10 s and were referenced to adamantane. Ramped-amplitude CP was used to minimize intensity variations of the nonprotonated aromatic carbons that are sensitive to Hartmann–Hahn mismatch at higher MAS rotation rates.<sup>33</sup> CP experiments were carried out at room temperature using a 5 ms contact time, spinning rate of 6 kHz, and a pulse repetition rate of 1.0 s.

Raman spectroscopy was performed using the 2.54 eV (488 nm) line of an Ar ion laser and the 1.96 eV (632.8 nm) line of a HeNe laser. The backscattered light was analyzed with a Jobin Yvon 270M spectrometer equipped with a liquid-nitrogen-cooled Spectrum One CCD and a holographic notch filter. A Nikon 55 mm camera lens was employed both to focus the beam on the sample and to collect the scattered light. Averaging three 30 s scans was sufficient to obtain high-resolution Raman spectra.

**2.2. Preparation of  $\text{H}_2\text{SO}_4$  Protonated SWNTs.** Purified SWNTs (3 mg) were placed in 15 mL of concentrated sulfuric acid ( $\sim 96\%$ , J. T. Baker) and sonicated in a water bath sonicator (Bransonic Ultrasonic Cleaner, 1510) for 5 min at room temperature. The mixture was heated to 80 °C and stirred for 24 h. The protonated nanotubes were isolated via suction filtration on a 1.0  $\mu\text{m}$  PTFE membrane and air-dried for 3 h at room temperature. The protonated SWNTs were neutralized by soaking in 6 M NaOH (J. T. Baker) for 18 h at room temperature. The neutralized nanotubes were isolated by suction filtration.

**2.3. Preparation of SWNT–Nafion Composites.** SWNT–Nafion composites were prepared from dispersions of SWNTs in a 5 wt % Nafion-1100 solution containing lower aliphatic alcohols and water (Aldrich) as reported previously.<sup>27,28</sup> Purified SWNTs were added to the Nafion solution to achieve a 1 wt % nanotube loading in the final composite membrane. The SWNT material was dispersed using a cup-horn sonicator driven by an ultrasonic processor (Cole-Palmer, 750 W). The mixture was cooled to 15 °C with a water bath during

(29) Dillon, A. C.; Gennett, T.; Jones, K. M.; Alleman, J. L.; Parilla, P. A.; Heben, M. J. *Adv. Mater.* **1999**, *11*, 1354–1358.

(30) Thess, A.; Lee, R.; Nikolaev, P.; Dai, H. J.; Petit, P.; Robert, J.; Xu, C. H.; Lee, Y. H.; Kim, S. G.; Rinzler, A. G.; Colbert, D. T.; Scuseria, G. E.; Tomanek, D.; Fischer, J. E.; Smalley, R. E. *Science* **1996**, *273*, 483–487.

(31) Gilbert, K. E. H. Purification and Gas Adsorption Studies of Single-walled Carbon Nanotubes. Thesis, Colorado School of Mines, Golden, CO, 2005.

(32) Liu, L.; Fan, S. S. *J. Am. Chem. Soc.* **2001**, *123*, 11502–11503.

(33) Metz, G.; Wu, X.; Smith, W. O. *J. Magn. Reson., Ser. A* **1994**, *110*, 219–227.



ultrasonication (30 min). The resulting suspension was placed in a water bath sonicator (Bransonic Ultrasonic Cleaner, 1510) for 18 h at room temperature. Thin films were cast onto a Bytac substrate and dried in vacuo (100 mTorr) for 18 h at room temperature. The resulting SWNT–Nafion composite films were removed from the casting plate and dried in vacuo ( $1 \times 10^{-8}$  Torr) for an additional 72 h at 70 °C.

SWNT–Nafion composites were neutralized by immersing the films into a 6 M NaOH solution (J. T. Baker) for 48 h at room temperature. The neutralized films were isolated via suction filtration and dried in an oven at 70 °C for 18 h. Partially neutralized SWNT–Nafion composites were formed when the isolated neutralized material was washed with  $3 \times 300$  mL of water and then dried in an oven at 70 °C for 18 h.

**2.4. Exposure of SWNTs to Water.** In a typical experiment, purified SWNTs (2 mg) were placed in 10 mL of water. The resulting suspension was placed in a water bath sonicator (Bransonic Ultrasonic Cleaner, 1510) for 20 h at room temperature. The material was isolated via suction filtration on a 1.0  $\mu\text{m}$  PTFE membrane.

**2.5. Preparation of SWNT–AQ55 Composites.** The SWNT–AQ55 composites were prepared as described above for the SWNT–Nafion composites. The AQ55 polymer (Eastman Chemical Co.) was dissolved in a 25% ethanol solution (aqueous) to obtain a 5 wt. % polymer solution. The SWNT percent by weight was adjusted accordingly to achieve a 1 wt % loading in the final composite.

### 3. Results and Discussion

**3.1. Raman Spectroscopy of Protonated SWNTs in Sulfuric Acid and Nafion.** Prior to discussing the NMR results, we first report Raman spectroscopy evidence for the reversible protonation of the SWNT surfaces in sulfuric acid and Nafion. Raman scattering has been used extensively to study the interaction of SWNTs with alkali metals<sup>34–36</sup> and strong acids.<sup>18,20–22,29</sup> Figure 2 shows Raman spectra for pristine SWNTs, SWNTs treated in  $\text{H}_2\text{SO}_4$  before and after neutralization in NaOH, and SWNTs encapsulated in Nafion before and after neutralization with NaOH, acquired with excitation energies ( $E_{\text{laser}}$ ) of 2.54 eV (left panel) and 1.96 eV (right panel). The two excitation energies, 2.54 and 1.96 eV, were chosen to probe predominantly the  $E_{33}^{\text{S}}$  and  $E_{11}^{\text{M}}$  interband transitions, respectively, of the semiconducting and metallic tubes present in the 1.1–1.4 nm diameter distribution of our laser-generated SWNT material.<sup>21,37–38</sup> The Raman spectrum of the pristine SWNTs at  $E_{\text{laser}} = 2.54$  eV shows the familiar resonantly enhanced G-band peaked at  $1583\text{ cm}^{-1}$  due to the carbon–carbon translational modes. The spectrum is typical of the low defect density purified SWNT materials employed here.<sup>39,40</sup> For example, the D-band feature at  $1340\text{ cm}^{-1}$  shown in the inset has a fwhm of only  $19\text{ cm}^{-1}$  and a  $D/G$  ratio of 1/160 at 2.54 eV excitation. The spectrum of the pristine SWNTs taken at 1.96 eV excitation shows the characteristic lower frequency G-band feature at  $1533\text{ cm}^{-1}$  with a Breit–Wigner–Fano (BWF) line shape as well as the high energy mode at  $1577\text{ cm}^{-1}$  as expected for Raman scattering from metallic SWNTs.

Treatment in sulfuric acid blue shifts the G-band by  $\sim 23\text{ cm}^{-1}$  such that the high-energy feature is located at 1606 and  $1599\text{ cm}^{-1}$  for 2.54 and 1.96 eV excitations, respectively (Figure 2). Consistent with the charge polarization expected for the formation of a  $\text{C:H}^+$  moiety, the carbon bonds are stiffened due to a reduction in the delocalized electron density on the SWNT. A blue shift of a similar magnitude has been reported by Ramesh et al. for SWNTs in chlorosulfonic acid.<sup>18</sup> The acid-solubilized SWNTs were described as protonated polycarbonocations that were charged balanced by the conjugate base anions. These authors calculated that a shift of  $23\text{ cm}^{-1}$  corresponds to a single positive charge being shared over  $\sim 14$  carbons using data from Sumanasekera et al.<sup>41</sup> Most notable in our data is the complete absence of the BWF line shape with  $E_{\text{laser}} = 1.96$  eV after the sulfuric acid treatment. The loss of the BWF line shape can be qualitatively understood as being due to the removal of electron density or, conversely, the injection of positive charge. In previous studies,<sup>20,21</sup> similar observations were explained in terms of a loss in resonance enhancement due to a shift in the Fermi level induced by p-type doping with  $\text{H}_2\text{SO}_4$ . More recent studies consider that debundling alone can diminish the intensity of the BWF line shape contribution.<sup>42,43</sup> The protonation in sulfuric acid is evidently reversible when the nanotube sidewalls are treated with NaOH. The data in Figure 2 show that the vibrational modes soften and the lineshapes of the pristine tubes are regained after deprotonation in base. In fact, the Raman spectra after neutralization are virtually indistinguishable from those of the pristine SWNTs. As previously reported,<sup>18</sup> the SWNTs were not damaged by the acidic conditions. The D-band intensity was unchanged after neutralization (not shown) indicating little or no net conversion of  $\text{sp}^2$  to  $\text{sp}^3$  bonding and few, if any, new defects added to the SWNTs<sup>40</sup> during the acidification and neutralization procedures. These results add support to the conclusion that no C–H or C–O bonds are formed during protonation.

Figure 2 also shows typical Raman spectra for the SWNT–Nafion composites before and after neutralization in base. The Raman data at  $E_{\text{laser}} = 2.54$  eV show a loss in G-band intensity consistent with protonation, but the principal peak at  $1583\text{ cm}^{-1}$  is not significantly shifted relative to the spectrum for pristine tubes. In contrast, at  $E_{\text{laser}} = 1.96$  eV, which primarily probes the metallic tubes in the distribution, the BWF mode is absent and the main G-band peak is upshifted  $6\text{ cm}^{-1}$  relative to the pure tube Raman data. These data, coupled with the observation that Nafion is capable of debundling nanotubes,<sup>27,28</sup> indicate that the sulfonic acid groups on the perfluorosulfonated backbone of Nafion are capable of protonating the SWNTs in similarity to sulfuric acid. The degree of protonation is smaller than with concentrated sulfuric acid presumably due to the lower concentration of acidic sites in Nafion. The  $6\text{ cm}^{-1}$  blue shift in the G-band indicates a reduction in electron density on the nanotube of  $\sim 0.02\text{ e}^-/\text{C}$ .<sup>41</sup> As with sulfuric acid, the protonation of the nanotube sidewalls was completely reversible in Nafion. Once the SWNT–Nafion composites were neutralized with a competing base, sodium hydroxide, the Raman spectroscopy features of the pristine tubes were for the most part restored

(34) Claye, A.; Rahman, S.; Fischer, J. E.; Sirenko, A.; Sumanasekera, G. U.; Eklund, P. C. *Chem. Phys. Lett.* **2001**, *333*, 16–22.

(35) Rao, A. M.; Eklund, P. C.; Bando, S.; Thess, A.; Smalley, R. E. *Nature* **1997**, *388*, 257–259.

(36) Gupta, S.; Hughes, M.; Windle, A. H.; Robertson, J. J. *Appl. Phys.* **2004**, *95*, 2038–2048.

(37) Oron-Carl, M.; Hennrich, F.; Kappes, M. M.; Lohneysen, H. v.; Krupke, R. *Nano Lett.* **2005**, *5*, 1761–1767.

(38) Hennrich, F.; Krupke, R.; Lebedkin, S.; Arnold, K.; Fischer, R.; Resasco, D. E.; Kappes, M. M. *J. Phys. Chem. B* **2005**, *109*, 10567–10573.

(39) Dillon, A. C.; Yudasaka, M.; Dresselhaus, M. S. *J. Nanosci. Nanotechnol.* **2004**, *4*, 691–703.

(40) Dillon, A. C.; Parilla, P. A.; Alleman, J. L.; Gennett, T.; Jones, K. M.; Heben, M. J. *Chem. Phys. Lett.* **2005**, *401*, 522–528.

(41) Sumanasekera, G. U.; Allen, J. L.; Fang, S. L.; Loper, A. L.; Rao, A. M.; Eklund, P. C. *J. Phys. Chem. B* **1999**, *103*, 4292–4297.

(42) Jiang, C. Y.; Kempa, K.; Zhao, J. L.; Schlecht, U.; Kolb, U.; Basche, T.; Burghard, M.; Mews, A. *Phys. Rev. B* **2002**, *66*, 161404.

(43) Paillet, M.; Poncharal, P.; Zahab, A.; Sauvajol, J. L.; Meyer, J. C.; Roth, S. *Phys. Rev. Lett.* **2005**, *94*, 237401.

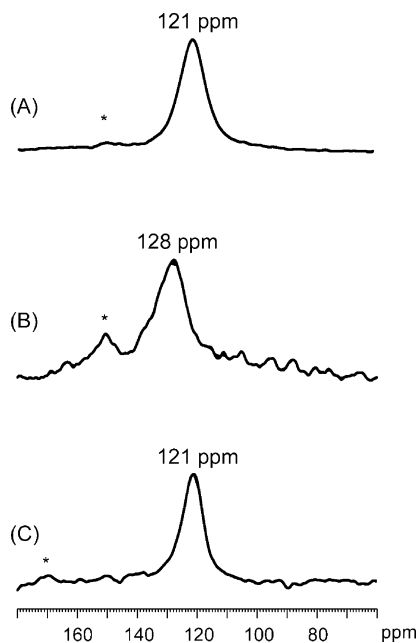


**Figure 3.** Solid-state MAS  $^{13}\text{C}$  NMR data for (A) pristine SWNTs, (B) SWNTs protonated by  $\text{H}_2\text{SO}_4$ , and (C) SWNTs protonated by  $\text{H}_2\text{SO}_4$  and then neutralized with NaOH. The asterisks indicate spinning sidebands from the polyethylene plugs. Each spectrum was acquired over  $\sim 11$  h.

(Figure 2). The neutralized SWNT–Nafion composites exhibit a narrower BWF line shape relative to pure SWNTs at  $E_{\text{laser}} = 1.96$  eV, consistent with the bundle sizes being smaller in the Nafion matrix (vide infra).

**3.2.  $^{13}\text{C}$  NMR of SWNTs Reversibly Protonated in  $\text{H}_2\text{SO}_4$  and Nafion.** Recent advances in solid-state NMR methods have enabled researchers to clarify structure and dynamics with respect to noncovalent interactions in molecular systems, e.g., hydrogen bonding and  $\pi$ – $\pi$  interactions.<sup>4,44</sup> Thus, NMR is an ideal probe for the reversible protonation of SWNTs. As mentioned previously, the application of NMR to the analysis of SWNTs has been hindered by the lack of high-quality and high-purity carbon nanotube samples. Anisotropic interactions, e.g., the chemical shift anisotropy and dipolar couplings, and large magnetic inhomogeneities caused by residual metal catalyst from the growth process lead to a broadening of the isotropic  $^{13}\text{C}$  NMR signal for SWNTs.<sup>8</sup> The line broadening due to the chemical shift anisotropy and  $^{13}\text{C}$ – $^{13}\text{C}$  dipolar couplings can be removed by spinning the sample at the “magic angle” of  $54.7^\circ$ . In our NMR experiments, the magnetic inhomogeneities were minimized by using a laser vaporization growth process and a purification method that efficiently removed residual metal catalyst impurities to yield highly pure SWNT material.<sup>29–31</sup> Figure 3a shows  $^{13}\text{C}$  NMR resonance at 121 ppm for these highly pure SWNTs. Such a  $^{13}\text{C}$  chemical shift is consistent with previous reports for SWNT samples.<sup>6–12,16</sup> The fwhm was measured to be only 10 ppm, confirming that the SWNT material has a low metal content and few defects as compared to unpurified SWNT material.<sup>9</sup> The 10 ppm line width may be attributed to the polydispersity in nanotube diameter and chirality or to the distribution of environments for nanotubes in different sized bundles. These laser-generated samples are known by fluorescence excitation spectroscopy to contain at least 15

different semiconducting tube species in the diameter range of 1.2–1.4 nm.<sup>45</sup> Coupled with the fact that 1/3 of all tubes in a given sample are likely to be metallic and nonemissive in fluorescence measurements,<sup>46</sup> as many as 23 different nanotube species may be present. In addition, transmission electron microscopy of the purified laser-generated SWNT samples shows nanotube bundles ranging in size from 30 to 150 nm.

Figure 3b shows the MAS  $^{13}\text{C}$  NMR data for purified SWNTs treated with concentrated  $\text{H}_2\text{SO}_4$ . The protonated nanotube carbons exhibit a  $^{13}\text{C}$  resonance at 128 ppm that is shifted to higher frequency by 7 ppm relative to pure SWNTs. The NMR shift to higher frequency is similar to that seen for carbon nuclei in delocalized  $\pi$ -carbonium ions and in conducting polymers.<sup>44</sup> For example, in the case of polyacetylene, where chemical doping produces metallic behavior, the shift to higher frequency is attributed to the removal of electrons from the  $\pi$  system of the polymer.<sup>44</sup> Therefore, consistent with previously discussed Raman spectroscopy observations, we assign the primary cause of the shift to higher ppm to be the withdrawal of electronic charges from the SWNTs by the interaction with sulfuric acid. The broadness of the NMR signal and the appearance of shoulders reflects the dispersion of chemical shifts that could be due to differences in the degree of protonation and the resulting charge distributions for nanotubes inside and outside of bundles. SWNTs exhibit a lower solubility in  $\text{H}_2\text{SO}_4$  compared to other superacids such as chlorosulfonic acid.<sup>18</sup> Therefore, charge would not be distributed uniformly on all of the nanotube surfaces due to the incomplete delamination of nanotube bundles in  $\text{H}_2\text{SO}_4$ . However, it is important to note that all  $^{13}\text{C}$  resonances in the sample are significantly moved to higher frequency. As shown in Figure 3c, the  $^{13}\text{C}$  resonance returns to 121 ppm and the narrow line width is recovered upon neutralizing the  $\text{H}_2\text{SO}_4$ -protonated SWNTs with NaOH.

The MAS  $^{13}\text{C}$  NMR spectra for pure Nafion (Figure 4b) and neutralized Nafion (not shown) are dominated by a broad line at  $\sim 112$  ppm, which has been assigned to CF and  $\text{CF}_2$  structures in the polymer.<sup>47</sup> The MAS  $^{13}\text{C}$  NMR spectrum of the SWNT–Nafion composite (Figure 4c) shows this same feature as well as a signal due to SWNT  $^{13}\text{C}$  nuclei at 125 ppm. The  $^{13}\text{C}$  resonance for the nanotubes is notably broadened and shifted to higher frequency by 4 ppm relative to the NMR signal for pure SWNTs (Figure 4a). The shift in the  $^{13}\text{C}$  resonance for the SWNTs in the Nafion matrix indicates a change in the chemical environment of the nuclei comprising the nanotubes. As with the sulfuric acid case, and as seen by Raman spectroscopy, immersing the films in a 6 M NaOH solution reverses the protonation by Nafion. The neutralized composite exhibits a nanotube  $^{13}\text{C}$  NMR signal at 121 ppm (Figure 4d). Unfortunately, the SWNT signals could not be fully resolved in either the acidic or neutralized Nafion composites due to the overlapping CF and  $\text{CF}_2$  signals. A chemical shift for SWNT nuclei of 121 ppm in both pure SWNTs and the neutralized composite indicates that the fluorinated polymer backbone of Nafion does not significantly affect the bonding environment for SWNT nuclei.

**3.3.  $^1\text{H}$ – $^{13}\text{C}$  Cross Polarization NMR Analysis of SWNT Protonation in  $\text{H}_2\text{SO}_4$  and Nafion.** With clear evidence for

(45) McDonald, T. J.; Engtrakul, C.; Heben, M. J. Unpublished results.

(46) Bachilo, S. M.; Strano, M. S.; Kittrell, C.; Hauge, R. H.; Smalley, R. E.; Weisman, R. B. *Science* **2002**, *298*, 2361–2366.

(47) Liu, S. F.; Schmidt-Rohr, K. *Macromolecules* **2001**, *34*, 8416–8418.

(44) Clarke, T. C.; Scott, J. C.; Street, G. B. *IBM J. Res. Dev.* **1983**, *27*, 313–320.

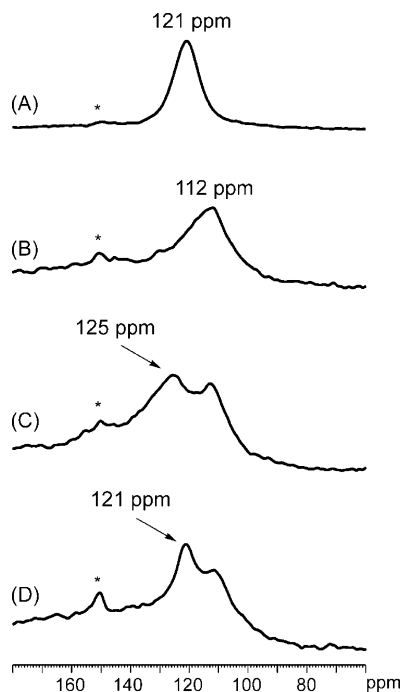


**Figure 4.** Solid-state MAS  $^{13}\text{C}$  NMR spectra of (A) pristine SWNTs, (B) pristine Nafion, (C) SWNT–Nafion composites, and (D) neutralized SWNT–Nafion composites. Peaks marked with asterisks are spinning sidebands from the polyethylene plugs. Each spectrum was acquired over  $\sim 11$  h.

protonation/deprotonation of SWNTs in  $\text{H}_2\text{SO}_4$  and Nafion, we next utilized  $^1\text{H}$ – $^{13}\text{C}$  CP-MAS to gain information pertaining to the proximity of protons and SWNT  $^{13}\text{C}$  nuclei in the protonated SWNT materials. The  $^1\text{H}$ – $^{13}\text{C}$  CP-MAS method has been used previously to study SWNTs<sup>10,11</sup> but has not yet been applied to the study of protonation of SWNTs. Figure 5a shows that a transfer of magnetization was indeed observed due to the dipolar interaction between the adsorbed protons and the carbons of the  $\text{H}_2\text{SO}_4$  protonated nanotubes. The  $^1\text{H}$ – $^{13}\text{C}$  CP-MAS signal at 128 ppm was fairly broad (fwhm  $\sim 14$  ppm) and shifted to higher frequency by 7 ppm relative to the  $^{13}\text{C}$  NMR signal for pure SWNTs (Figure 3a) in agreement with the  $^{13}\text{C}$  NMR data in Figure 3b. Similarly, the SWNT–Nafion composites displayed a CP signal at 125 ppm and a fwhm of  $\sim 17$  ppm (Figure 5b). Both CP spectra clearly show a distribution in chemical environments for the protonated nanotubes. Close inspection of the relatively broad lines reveals the presence of several shoulders that were difficult to observe in the  $^{13}\text{C}$  NMR data due to the overlapping Nafion signal. As previously discussed, these broad line widths most likely reflect differences in the degree of protonation for the various nanotubes distributed throughout the bundles. The CP approach offers an additional contrast mechanism that depends on the efficiency of magnetization transfer from protons to the SWNT  $^{13}\text{C}$  nuclei.

Initially, the SWNT–Nafion composites were neutralized with NaOH and washed with water to remove excess base. Unexpectedly, a broad  $^1\text{H}$ – $^{13}\text{C}$  CP-MAS signal at 122 ppm was still observed (Figure 5c), indicating that protons were still present close to the SWNT  $^{13}\text{C}$  nuclei. The pH of the water used to wash the composite was slightly acidic, and it has been shown that the  $\text{H}^+$  content in Nafion is sensitive to pH.<sup>48</sup> Thus,

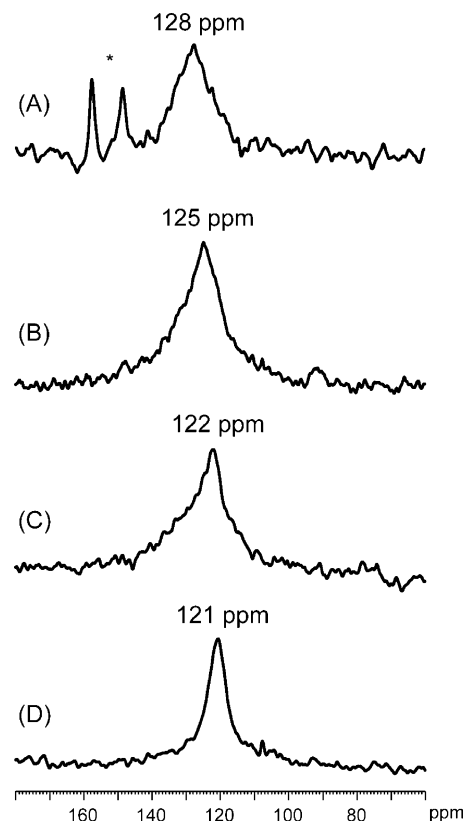


**Figure 5.**  $^1\text{H}$ – $^{13}\text{C}$  CP-MAS spectra for a (A) sulfuric acid protonated SWNTs (acquired over  $\sim 83$  h), (B) SWNT–Nafion composite (acquired over  $\sim 64$  h), (C) partially neutralized SWNT–Nafion composite (acquired over  $\sim 51$  h), and (D) fully neutralized SWNT–Nafion composite (acquired over  $\sim 83$  h). The asterisk indicates the spinning sidebands from an internal reference adamantane.

it is likely that the Nafion polymer was reprotonated to some degree resulting in the partial reprotonation of proximal nanotubes. The protonation of nanotubes has been shown to be sensitive to pH, with metallic nanotubes being the most reactive and protonating near neutral pH, followed by semiconducting nanotubes at more acidic pH values.<sup>22</sup> Therefore, a partial reprotonation of metallic nanotubes could explain why the line width of the signal for the SWNTs in Figure 5c was broad and not completely shifted back to the 121 ppm value observed for pure SWNTs. As previously mentioned, broad nanotube  $^{13}\text{C}$  NMR signals have been assigned to the dispersion of chemical shifts for carbon signals from semiconducting and metallic SWNTs.<sup>9,14,16</sup> Alternatively, a broad  $^{13}\text{C}$  NMR signal in Figure 5c would be expected if only the outer surface of the nanotube bundles were reprotonated in the partially neutralized SWNT–Nafion composites, leaving the interior tubes in the bundle unchanged.

The CP spectrum in Figure 5d was obtained after the SWNT–Nafion composites were soaked in 6 M NaOH and not washed with water. The  $^1\text{H}$ – $^{13}\text{C}$  CP-MAS signal for the fully neutralized composite was observed at 121 ppm with a fwhm of only 6 ppm. Evidently, the water molecules retained in the polymer to hydrate the Na-exchanged sites<sup>49</sup> are sufficient to permit transfer of magnetization from protons to the SWNT  $^{13}\text{C}$  nuclei. The narrower line width of the signal relative to the 10 ppm width for pure SWNTs could mean that nanotubes in the Nafion matrix

(48) Okada, T.; Satou, H.; Okuno, M.; Yuasa, M. *J. Phys. Chem. B* **2002**, *106*, 1267–1273.

(49) James, P. J.; Elliott, J. A.; J., M. T.; Newton, J. M.; Elliot, A. M. S.; Hanna, S.; Miles, M. J. *J. Mater. Sci.* **2000**, *35*, 5111–5119.



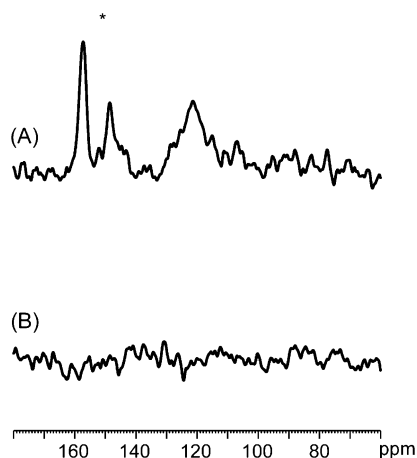


**Figure 6.**  $^1\text{H}$ – $^{13}\text{C}$  CP-MAS spectra of SWNTs (A) sonicated (acquired over  $\sim 22$  h) and (B) soaked (acquired over  $\sim 18$  h) in water. The  $^{13}\text{C}$  resonance for SWNTs is 121 ppm as seen in spectrum A. The asterisk indicates spinning sidebands from an internal reference adamantane.

are more effectively dispersed and, therefore, in a more homogeneous environment. We previously reported a 5-fold reduction for SWNT bundle sizes in SWNT–Nafion composites relative to purified SWNTs.<sup>27</sup> Transmission electron microscopy studies verify that the bundle sizes are unchanged after neutralization. The width of the SWNT resonance is also observed to be narrow by subtracting the  $^{13}\text{C}$  Nafion spectrum (Figure 4b) from the spectrum for the neutralized SWNT composite (Figure 4d), but the finding is more clearly observed in the CP spectrum in Figure 5d. Therefore, consistent with the Raman spectroscopy observations discussed previously (Figure 2), the 5-fold reduction in SWNT bundle size found in the SWNT–Nafion composites is likely reflected in the narrower  $^{13}\text{C}$  line shape (Figure 5d).

**3.4.  $^1\text{H}$ – $^{13}\text{C}$  Cross Polarization NMR of SWNTs Interacting with Water.** To further probe the role of water in magnetization transfer from protons to SWNT  $^{13}\text{C}$  nuclei, pure SWNTs were agitated in water for 20 h in a bath sonicator at room temperature. Figure 6a shows the  $^1\text{H}$ – $^{13}\text{C}$  CP-MAS spectrum with a weak, broad signal at 121 ppm as expected for a  $^{13}\text{C}$  resonance for pristine SWNTs. For comparison, a sample of SWNTs soaked in water for the same amount of time showed no  $^1\text{H}$ – $^{13}\text{C}$  CP-MAS signal (Figure 6b). It should be noted that an equivalent sonication experiment done instead with deuterium oxide also did not show a CP signal for the carbon nanotubes. The ultrasonic agitation evidently provided sufficient energy to enable water species to penetrate the purified SWNT paper to some degree whereas soaking did not. Although these purified nanotubes are strongly hydrophobic on the macroscale, there are both molecular simulation and experimental data that support the adsorption of water on carbon nanotubes.<sup>50–56</sup> Recently, it

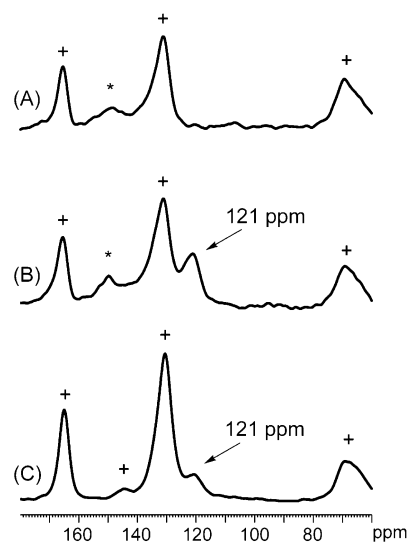


**Figure 7.**  $^{13}\text{C}$  NMR spectra (acquired over  $\sim 11$  h) of (A) the AQ55 polymer and (B) SWNT–AQ55 composites and  $^1\text{H}$ – $^{13}\text{C}$  CP-MAS spectrum of the (C) SWNT–AQ55 composite (acquired over  $\sim 2$  1/2 h). Spinning sidebands from the polyethylene plugs are indicated by asterisks, and the plus signs indicate the  $^{13}\text{C}$  resonances from the AQ55 polymer.

has been shown by  $^2\text{H}$  NMR that deuterium is able to attach to carbon nanotubes from deuterated water solutions after brief sonication.<sup>50,51</sup> As with our findings with respect to protonation with acids, the authors were careful to specify that C–D bonds were not observed. In our case, Raman spectroscopy confirmed that defects were not introduced by the sonication of the SWNTs in water. Since water is not known to delaminate nanotube bundles, and our samples are not purposefully cut, opened, or shortened, it is likely that the adsorbed water molecules giving rise to the CP signal are present on exposed surfaces, in grooves, or interstitial sites between nanotubes. Future work will involve using the CP technique to probe the adsorption of species as the SWNT material is processed to change the number density of groove, interstitial, and interior sites. Also, the CP technique should be useful for probing the interaction of nanotubes with water under different pH conditions.

**3.5.  $^{13}\text{C}$  and  $^1\text{H}$ – $^{13}\text{C}$  Cross Polarization NMR Studies of SWNT–AQ55 Composites.** To further explore the interactions between SWNTs and a polymer backbone, we combined SWNTs with AQ55, a polymer containing an alkyl backbone (Figure 1). The AQ55 polymer is a linear polyester polymer that contains polar sulfonate groups attached to the hydrophobic C–H polymer backbone. Such polymers are not superacids but have the ability to solubilize SWNTs by wrapping around the SWNT to create stable dispersions at pH 6 to 7.<sup>57</sup> The  $^{13}\text{C}$  NMR spectrum of the neat AQ55 polymer is shown in Figure 7a. In Figure 7b, the NMR spectrum of the SWNT–AQ55 composite exhibits the features of the neat AQ55 polymer with an additional  $^{13}\text{C}$  NMR signal at 121 ppm due to the nanotube carbons.

Figure 7c shows the  $^1\text{H}$ – $^{13}\text{C}$  CP-MAS spectrum for the SWNT–AQ55 composite. The clear observation of a  $^1\text{H}$ – $^{13}\text{C}$  CP-MAS signal for both the AQ55 and the SWNTs shows close contact between protons and  $^{13}\text{C}$  nuclei for both materials. On the basis of the signal-to-noise and acquisition time of the

- (50) Fu, K. F.; Kitaygorodskiy, A.; Rao, A. M.; Sun, Y. P. *Nano Lett.* **2002**, *2*, 1165–1168.  
 (51) Fu, K. F.; Li, H. P.; Zhou, B.; Kitaygorodskiy, A.; Allard, L. F.; Sun, Y. P. *J. Am. Chem. Soc.* **2004**, *126*, 4669–4675.  
 (52) Ohba, T.; Kanoh, H.; Kaneko, K. *J. Am. Chem. Soc.* **2004**, *126*, 1560–1562.  
 (53) Walther, J. H.; Jaffe, R.; Halicioglu, T.; Koumoutsakos, P. *J. Phys. Chem. B* **2001**, *105*, 9980–9987.  
 (54) Ellison, M. D.; Good, A. P.; Kinnaman, C. S.; Padgett, N. E. *J. Phys. Chem. B* **2005**, *109*, 10640–10646.  
 (55) Ghosh, S.; Ramanathan, K. V.; Sood, A. K. *Europhys. Lett.* **2004**, *65*, 678–684.  
 (56) Kolesnikov, A. I.; Zanotti, J. M.; Loong, C. K.; Thiyagarajan, P.; Moravsky, A. P.; Loutfy, R. O.; Burnham, C. J. *Phys. Rev. Lett.* **2004**, *93*, 035503.

- (57) O’Connell, M. J.; Boul, P.; Ericson, L. M.; Huffman, C.; Wang, Y. H.; Haroz, E.; Kuper, C.; Tour, J.; Ausman, K. D.; Smalley, R. E. *Chem. Phys. Lett.* **2001**, *342*, 265–271.

spectrum in Figure 7c, a significant enhancement in the carbon magnetization for both the polymer and SWNTs is observed as compared to Figure 7a,b. The C–H backbone of the AQ55 polymer is evidently efficient at transferring magnetization to the carbon nanotube surface due to the AQ55 polymer being wrapped around and in intimate contact with the surface of the SWNT. The carbon resonance of SWNTs for the SWNT–AQ55 composites was once again at 121 ppm reflecting no significant chemical interaction or change in the chemical environment of the carbon nuclei of the SWNTs. These data, coupled with the lack of a change in the 121 ppm  $^{13}\text{C}$  NMR signal for the neutralized SWNT–Nafion composites, demonstrates that the interaction between nanotubes and nonpolar polymer backbones is relatively weak.

#### 4. Conclusion

In summary, we have characterized protonation and deprotonation of  $^{13}\text{C}$  isotope-labeled SWNTs using solid-state NMR and Raman spectroscopy. Both sulfuric acid and Nafion protonate the nanotube sidewalls creating a different local environment for carbon nuclei and causing the  $^{13}\text{C}$  NMR signal to shift to higher frequency. The chemistry of the protonation is described as a charge-transfer process and the formation of a  $\text{C}:\text{H}^+$  moiety. Fractional electronic charge is withdrawn from the nanotube at the site of protonation to stabilize the interaction.<sup>18</sup> The notable deshielding of the  $^{13}\text{C}$  NMR signals for

protonated SWNTs is consistent with previous experimental work indicating that the electronic properties of carbon nanotubes are extremely sensitive to pH.<sup>22,58</sup> The chemical shift for the nanotubes was sensitive to the amount of positive charge dispersed on the nanotubes as measured by Raman spectroscopy. The protonation reactions were also observed in  $^1\text{H}$ – $^{13}\text{C}$  CP-MAS studies. The CP studies with neutralized SWNT–Nafion composites and water adsorbed on the SWNTs revealed that the presence of water without protonation was sufficient to yield a CP spectrum. The  $^{13}\text{C}$  chemical shifts for SWNTs in neutralized Nafion and AQ55 polymers were not affected by interactions with either of the polymer backbones. The  $^{13}\text{C}$  NMR and  $^1\text{H}$ – $^{13}\text{C}$  CP-MAS data for carbon nanotubes exhibited variations in line width and chemical shift due to the different physical and chemical environments.

**Acknowledgment.** This work was supported by the U.S. Department of Energy (DOE) Solar Photochemistry program funded by the Office of Science, Office of Basic Energy Sciences, Division of Chemical Sciences, Geosciences, and Biosciences.

JA0557886

(58) Dukovic, G.; White, B. E.; Zhou, Z. Y.; Wang, F.; Jockusch, S.; Steigerwald, M. L.; Heinz, T. F.; Friesner, R. A.; Turro, N. J.; Brus, L. E. *J. Am. Chem. Soc.* **2004**, *126*, 15269–15276.